Mansoura University
Faculty of Engineering
Mansoura Engineering Journal

The Influence of Flight Height and Overlap on UAV Imagery Over Featureless Surfaces

Ahmed Elhadary*, Mostafa Rabah, Essam Ghanim, Rasha Mohie and Ahmed Taha

KEYWORDS:
UAV flight configuration, flight altitude effect, overlap ratio, non-textured surface

***Abstract*— The improvement of Unmanned Aerial System (UAS) and photogrammetric computer vision (CV) algorithms have presented an aerial imaging technique for high accuracy and low-cost alternatives for mapping and topographic applications. Structure from motion (SFM) is an automation photogrammetric CV algorithm used for generating 3D colored point clouds and 3D models from overlapping images. One of the biggest problems preventing the automation extraction and matching key points in the aligning aerial images is the featureless surface of the covered area. This paper assessed the effect of flight altitude and overlap ratio on 3D point clouds' geometric accuracy and models produced by Unmanned Aerial Vehicle (UAV) images captured over non-textured sandy areas. Four different flight altitudes (140 m, 160 m, 180 m, and 200m) related to spatial resolution (3.41, 3.9, 4.39, 4.68 cm/pix GSD), respectively and three different overlap levels (60 %, 70 %, and 80 %) were assessed using RGB images captured by UX5 UAV over a non-textured sandy area in Jahra, Kuwait. The results showed that altitude increment might reduce flight time, processing time, and cost with keeping the acceptable and suitable geometric accuracy. The different UAV altitudes 140, 160, 180, and 200 m AGL gave geometric accuracy 0.043, 0.049, 0.052, and 0.057 m for IG process and 0.036, 0.039, 0.048, and 0.053 m for DG process, respectively. The increasing of image overlap ratio from 60 % to 80 % leads to an increase in photogrammetric point clouds' geometric accuracy from 0.685m to 0.049 m for IG process. Generally, favorable results are obtained for the four different altitudes and overlap ratios of 80 % at least.**

I. INTRODUCTION

UNLIKE conventional topographic survey techniques and satellite imagery, images captured by UAVs have advantages of low platform cost, flexibility, rapid, high resolution, precise positioning, and no need for permissions in most countries. Based on these advantages, photogrammetry based on the UAV platform has become a popular technique in mapping topographic applications. Capturing imagery by a camera installed in UAV has importance in cartographic (Crommelinck et al., 2017), remote sensing (Aasen et al., 2018), agriculture (Borgogno Mondino and Gajetti, 2017), environmental (Manfreda et al., 2018), and metrology (Daakir et al., 2017) applications.

Received: (01 February, 2022) - Revised: (09 March, 2022) - Accepted: (15 March, 2022)

***Corresponding author**: Ahmed Elhadary, Assistant lecturer, Department of Civil Engineering, Benha Faculty of Engineering, Benha University, Egypt (e-mail: ahmed.elhadari@bhit.bu.edu.eg), (phone: 01097855964)*

Mostafa Rabah, Professor of Surveying and Geodesy, Department of Civil Engineering, Benha Faculty of Engineering, Benha University, Egypt (e-mail: mrabah@bhit.bu.edu.eg).

Essam Ghanim, Lecturer, Department of Civil Engineering, Benha Faculty of Engineering, Benha University, Egypt (e-mail: essam.ghanem@bhit.bu.edu.eg).

Rasha Mohie, Lecturer, Department of Civil Engineering, Benha Faculty of Engineering, Benha University, Egypt (e-mail: rasha.abdelfattah@bhit.bu.edu.eg).

Ahmed Taha, Lecturer, Department of Civil Engineering, Benha Faculty of Engineering, Benha University, Egypt (e-mail: ahmed.soliman@bhit.bu.edu.eg).

Using UAVs as a photogrammetric platform have the ability to overfly and capture wide accessible or inaccessible, or dangerous areas within a short time with high resolution due to the low altitude of flying. For the geomatics applications, a geo-referencing of the captured images is required to determine the points' 3D location in a certain reference system. There are two methods of determining the exterior orientation (EO) parameters for each image in aerial imaging. The first way is integrating the measurements from the differential global navigational satellite system (DGNSS) and the inertial measurement system. This technique is called direct geo-referencing (DG). The second way is the indirect geo-referencing (IG), which uses the good distribution of GCPs (Ground Control Points) to compute the EO parameters (Rabah, et al., 2018).

In addition to the processing parameters, UAV Photogrammetry output products' accuracy is affected by the field configuration like flight height which determines the pixel size of the images and defines the spatial quality, overlap, and side lap and distribution of GCPs (Mesas-Carrascosa et. al., 2016). There are some problems that affect the automatic matching and the efficiency of image processing. One of the biggest problems is the featureless surface, which prevents and affects the SIFT process (Taha et al., 2022). To overcome this problem, flight field configuration parameters must be taken into consideration before flight data acquisition.

The UAV altitude AGL (Above Ground Level) and ratio of image overlap affect the accuracy and efficiency of aligning and automatic matching step in the Scale-Invariant Feature Transform (SIFT) process. The image overlap offers enough corresponding points in sequence images to match and align them. The overlap ratio should be enough, or the photos can't be aligned. The effect of overlap is divided into two portions: the forward and the side overlap. The number of photos per second manages the forward overlap, and side overlap is managed in the flight planning (Falkner and Morgan, 2002).

$$o_{forward} = \left(1 - \frac{d_{forward} * f}{H * W}\right) * 100$$
$$o_{side} = \left(1 - \frac{d_{side} * f}{H * W}\right) * 100$$

Where:

$O_{forward}$: The forward overlap %, O_{side}: The side overlap %.
$d_{forward}$: The distance between two sequences images centers (m).
d_{side}: The distance between two successive flight lines (m).
f: The camera focal length (mm), W: The sensor width (mm).
H: The height of the camera above the ground (m).

The ground sampling distance (GSD) or spatial resolution is calculated by: $GSD = \frac{p}{f}H$, Where p is the pixel size on the sensor and GSD is the distance between two sequences pixels centers measured on the ground.

Domingo et al. (2019) assessed the influence of image resolution, camera type, and side overlap on models constructed from UAV data. The results showed that the accuracy increased when using finer image resolution and RGB camera. Seifert (2019) studied the effects of drone flight parameters on image reconstruction and successful 3D point extraction. Low flight altitudes yielded the highest reconstruction details and best precisions. Çelik et al. (2020) investigated the effect of flight height on DSM and orthophoto. Compared to a flight height of 50 meters, a more detailed and high-resolution model was created with 30 meters. As a result of this comparison, it was determined that the flight height should be determined according to the terrain structure, accuracy, precision, and time-cost balance expected from the job. From previous researches, although the featureless surface of the covered area surface is one of the biggest problems and obstacles of image processing, no articles discuss and study this parameter.

This paper aims to study the effect of flight altitude AGL and image overlap ratio on point extraction, matching, image reconstruction, and the geometric accuracy of 3D point clouds and models generated by UAV images over featureless flat areas. For understanding the influence of UAV variables on the precision of reconstruction detail and image matching parameters during IG and DG processing, this study explored six different flights:

1) Four different flight height AGL (140m, 160 m, 180 m, and 200 m) with image spatial resolution (3.41, 3.9, 4.39, and 4.68 cm/pix GSD), respectively.
2) Three levels of the image forward and lateral overlap (60 %, 70 %, and 80 %) using 160 m flight altitude.

The other purpose is forming mathematical formulas to predict the UAV point cloud's geometrical accuracy by changing the GSD cm/pix and image overlap ratio.

II. RESEARCH METHODOLOGY:

A. *Area of Study:*

The six different altitudes AGL and overlap ratio missions were performed on the part of the desert located in Jahra, Kuwait (centered at latitude = 29o 13' 4.54" N, longitude = 47o 39' 45.14" E), figure 1 shows the test area on Google maps.

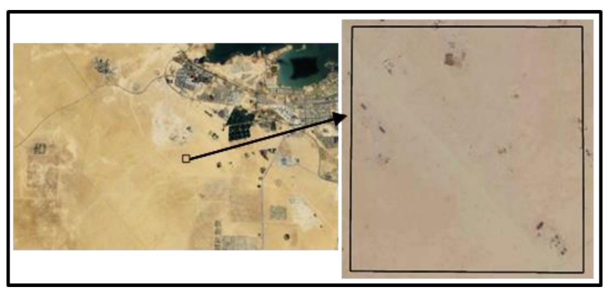

Fig. 1: The test area on Google maps.

B. *Photogrammetric Data Acquisition:*

Fig. 2: The used UX5 UAV and SONY camera.

The six Photogrammetric data acquisition has been performed of a different four height AGL, and three different overlap ratios with image format 6000 x 4000 pixels using 16 mm focal length SONY ILCE-5100 camera equipped a fixed-wing UAV UX5 vehicle with 1 m Wing length. Figure 2 shows the used UAV and camera, and Figure 3 shows a sample of the acquired images. The ground points are needed for geo-referencing the photogrammetric output products. 13 ground targets were set up, consisting of black-white square plates determined by static GNSS; figure 4 shows the identification of the ground points. Five points used as Ground control points (GCPs) were chosen in each corner and center, and the remaining eight points were used as independent checkpoints (ICPs); figure 5 shows the locations of the GCPS and ICPs.

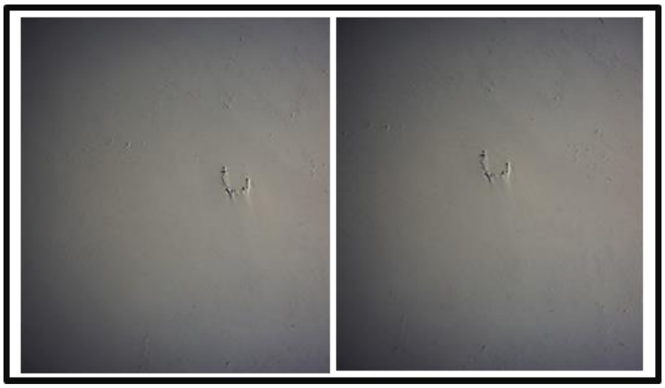

Fig. 3: Sample of the acquired UAV images

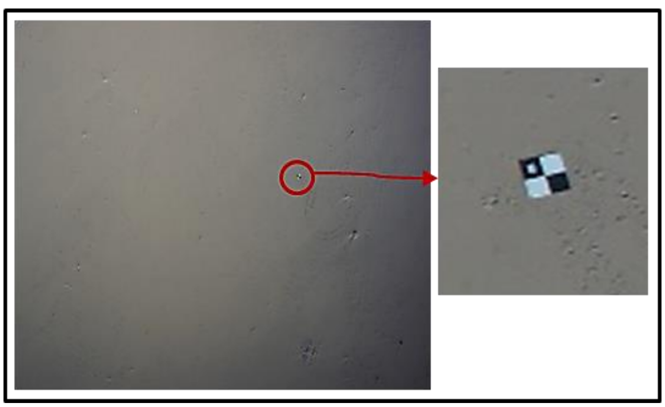

Fig. 4: The Identification of GCPs in images.

Six flights were planned to test the influence of the altitude AGL and image overlap ratio in the accuracy of processing UAV images covering featureless flat areas, as presented in figure 6. The six data acquisition is processed by the two techniques IG and DG by five GCPs determined by static GNSS and EO parameter determined by RTK-GNSS and eight ICPs used as checkpoints. All the flight missions were performed under the same parameters and wind conditions; thus, the accuracy of generated products is only dependent on flight altitude or overlap ratio.

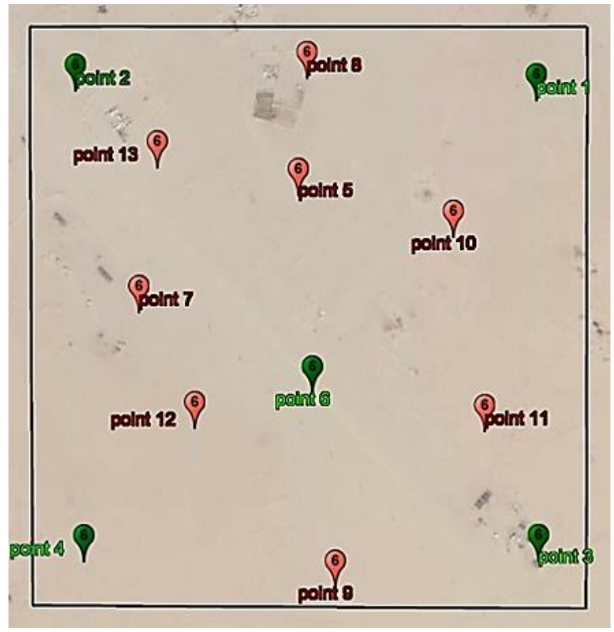

Fig. 5: The locations of 5 GCPs (Green mark) and 8 ICPs (Red mark).

C. Photogrammetric Data Processing:

After the photogrammetric missions are performed, the obtained UAV images are processed through Agisoft Metashape professional 1.6.0 software. The processing provides 3D colored point clouds, and 3D photogrammetric models of the study area. The process is performed in two main steps. Firstly, aligning and matching the images. Secondly, geo-referencing the images, as shown in figure 7, (Agisoft, 2019).

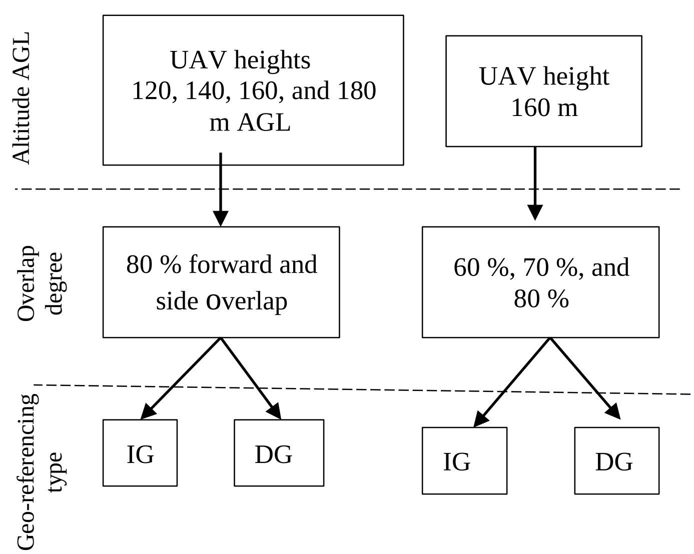

Fig. 6: Scheme of UAV field configuration and processing.

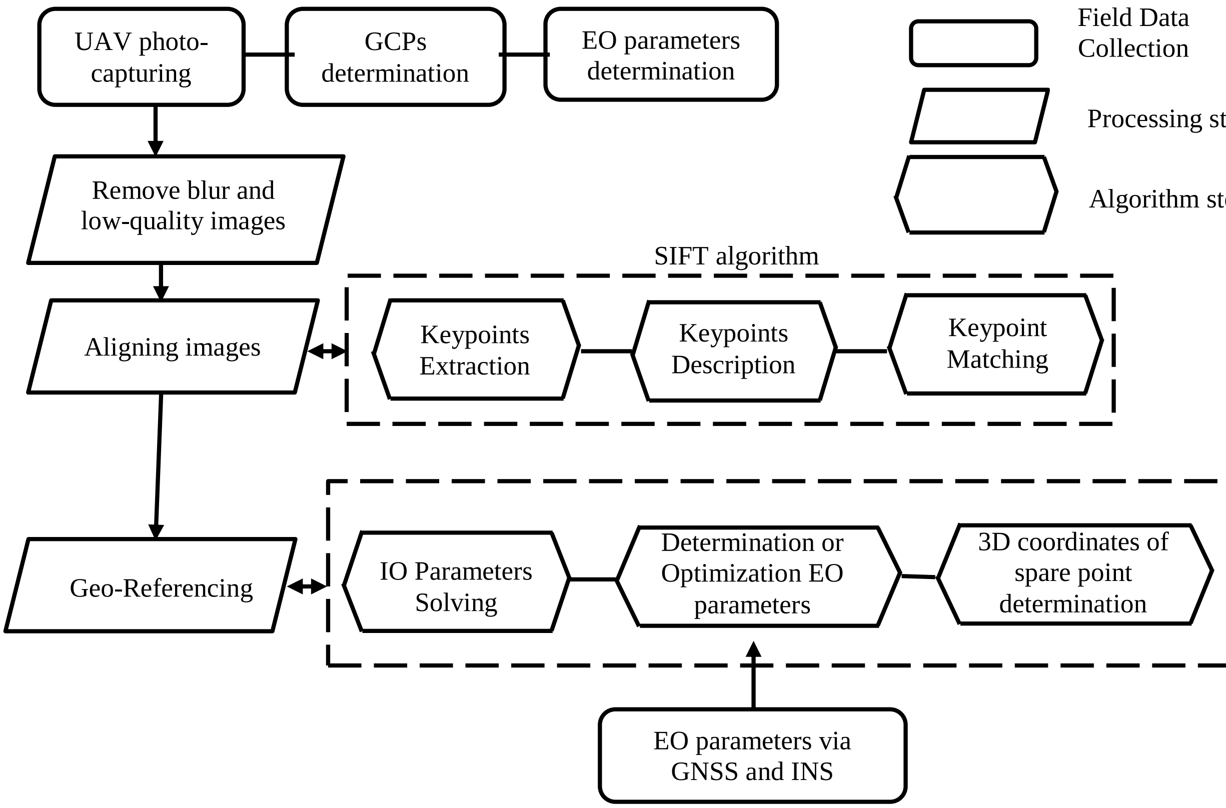

Fig. 7: Flowchart of field data collection and image processing stages.

III. RESULTS AND DISCUSSIONS

Six different missions, four different altitude AGL, and three different images overlap ratios as shown in figure 6, were tested and analyzed to show the effect of field configuration on the spatial accuracy of the generated point clouds by UAV featureless images. 13 ground points were measured by static GNSS, and RTK-GNSS determined the linear EO parameters for each image. For IG, five ground points were distributed regularly overall area used as GCPs and the remaining eight points used as ICPs to check the generated photogrammetric point clouds' geometric accuracy. For DG, the known linear EO parameters are used for geo-referencing without needing GCPs, and the same eight ICPs are used. Figure 5 shows the GCPs and ICPs locations. For checking geometric accuracy, Root Mean Square Error (RMSE) is determined for ICPs as a difference between the static GNSS and UAV data, (FGDC, 1998).

$$\mathrm{RMSE_X} = \sqrt{\frac{\sum(\mathrm{X_{GNSS}} - \mathrm{X_{UAV}})^2}{\mathrm{n}}}$$

$$\mathrm{RMSE_Y} = \sqrt{\frac{\sum(\mathrm{Y_{GNSS}} - \mathrm{Y_{UAV}})^2}{\mathrm{n}}}$$

$$\mathrm{RMSE_{XY}} = \sqrt{\mathrm{RMSE_X}^2 + \mathrm{RMSE_Y}^2}$$

$$\mathrm{RMSE_Z} = \sqrt{\frac{\sum(\mathrm{Z_{GNSS}} - \mathrm{Z_{UAV}})^2}{\mathrm{n}}}$$

$$\mathrm{RMSE_{XYZ}} = \sqrt{\mathrm{RMSE_X}^2 + \mathrm{RMSE_Y}^2 + \mathrm{RMSE_Z}^2}$$

A. The Effect of UAV Altitude AGL on UAV Featureless Images Processing:

To assess the influence of UAV flight configuration over a featureless surface for topographic applications. The impact of the UAV flight altitude AGL on both IG and DG processing was presented by studying four different heights (140, 160, 180, and 200 m) with a spatial resolution (3.41, 3.9, 4.39, and 4.68 cm/pix GSD) with 80 % for both forward and lateral overlap. Figure 8 shows the scheme of UAV flight heights and processing. The flight plan consisted of strips working east-west, and the flight planning parameters of the four different altitudes AGL are shown in table 1.

TABLE 1
THE FLIGHT PLANNING PARAMETERS OF THE FOUR DIFFERENT ALTITUDES AGL.

Flight altitude AGL (m)	No. of flight lines	No. of photos per line	No. of total photos	Flight time (minutes)
140	49	34	1666	34.5
160	43	30	1290	27
180	38	27	1026	21.5
200	35	25	875	18.5

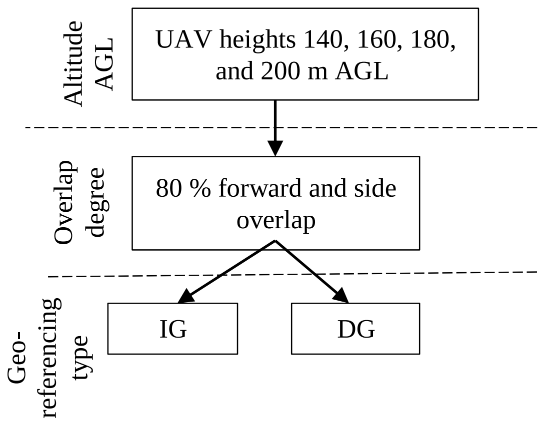

Fig. 8: Scheme of UAV flight heights and processing.

1. The influence of flight altitude on IG processing of featureless UAV images:

The four different altitude missions have been processed by IG processing using five GCPs and eight ICPs, as shown in figure 5. The geometric accuracy of easting, northing, and elevation is determined by calculating the RMSE of the eight ICPs from the selected flying height, shown in table 2 and figure 9.

TABLE 2
THE RMSE OF THE FOUR DIFFERENT ALTITUDE AGL OF IG PROCESS.

Flight height (m)	GSD (cm/pix)	Easting RMSE (m)	Northing RMSE (m)	Elevation RMSE (m)	Total RMSE (m)
140	3.41	0.023	0.015	0.033	0.043
160	3.9	0.012	0.028	0.038	0.049
180	4.39	0.017	0.03	0.039	0.052
200	4.68	0.022	0.032	0.042	0.057

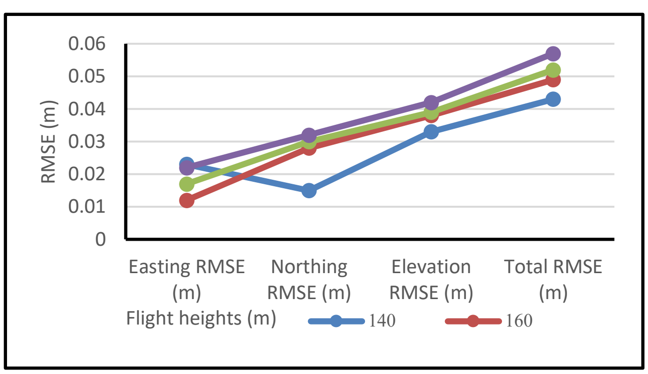

Fig. 9: The correlation between the attitude AGL and RMSE of the IG process.

Table 1 summarizes the results of the geometric accuracy related to flight heights where IG process was used. It is clear from figure 9 that the spatial accuracy is increased in northing and elevation directions whenever flying altitude is decreased. The highest geometric accuracy is obtained by the lowest flight altitude of 140 m AGL. Increasing the flight height leads to a decrease in the achieved geometric accuracy. The highest easting accuracy was gained by 160 m height, and both northing and elevation highest geometric accuracy were produced at 140 m flight height AGL. The four different altitudes gave a close total spatial accuracy within 0.043 to 0.057 m.

Table 3 shows the common matching parameters for the four different altitudes: spare point density, correct & wrong matching point, average tie point multiplicity, and matching time.

TABLE 3
THE MATCHING PARAMETERS OF THE FOUR DIFFERENT ALTITUDE AGL OF IG PROCESS.

Flight height (m)	140 m	160 m	180 m	200 m
Total points	227562	141767	127254	115342
Correct matching points	146453	87896	78357	62435
%Correct matching points	64.36 %	62 %	61.57 %	54.13 %
Wrong matching points	81109	53871	48897	52907
%Wrong matching points	35.64 %	38 %	38.43 %	45.87 %
Average tie point multiplicity	6.192	3.079	2.77	2.25
Matching time	1 day and 22 hours	1 day and 14 hours	1 day and 3 hours	20 hours and 35 minutes

Table 3 shows that the 140 m flight height AGL gave the highest-level spare point density, correct matching points, average tie point multiplicity, matching time, and lowest wrong matching points. Increasing the flight altitude leads to reduced spare point density, correct matching points, matching time, and average tie point multiplicity. At the altitude of 140 m, the largest images number (1666) at a ground sampling distance (resolution) of 3.41 cm/pixel were acquired. The generated point cloud with approximately 227562 3D points was extracted following the IG method. Generally, the increment of flight height can reduce flight and processing times and cost while keeping the acceptable geometric accuracy of the generated point clouds.

2. The effect of flight altitude on DG processing of featureless UAV images:

The four different altitudes AGL missions were processed by DG using the known linear EO parameters determined by RTK-GNSS without needing any GCPs. The eight ICPs were used for assessing the geometric accuracy of the generated point cloud. The RMSE of the eight ICPs was calculated for the three directions shown in table 4 and figure 10.

TABLE 4
THE RMSE OF THE FOUR DIFFERENT ALTITUDE AGL OF DG PROCESS.

Flight height (m)	GSD (cm/pix)	Easting RMSE (m)	Northing RMSE (m)	Elevation RMSE (m)	Total RMSE (m)
140	3.41	0.012	0.018	0.029	0.036
160	3.9	0.018	0.013	0.032	0.039
180	4.39	0.016	0.015	0.043	0.048
200	4.68	0.015	0.020	0.047	0.053

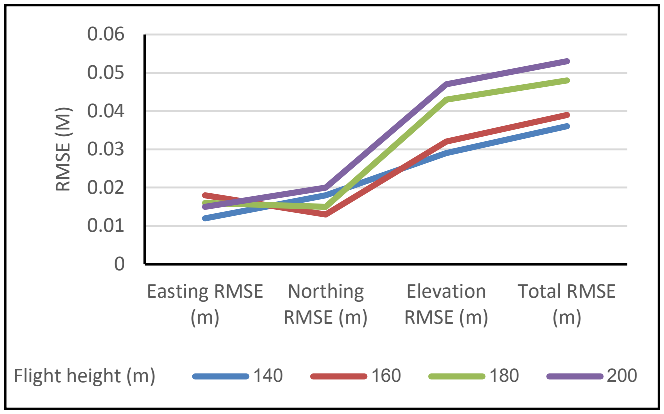

Fig. 10: The correlation between the attitude AGL and RMSE of DG process.

Based on table 4 and figure 10, As flight height AGL is increased, RMSE of the point cloud is increased. From 140 m AGL, flight gives a geometric accuracy of 0.036 m. from 160 m AGL, the RMSE was 0.039 m. from 180 m AGL, the RMSE was 0.048 m. RMSE was 0.053 m at altitude of 200 m AGL. This result shows that when the altitude AGL increases, image GSD also increases, affecting incrementing the RMSE.

Table 5 shows the correlation between the flight height AGL and the matching parameters represented in the point density, correct & wrong matching points, average tie point multiplicity, and matching time.

TABLE 5
THE MATCHING PARAMETERS OF THE FOUR DIFFERENT ALTITUDE AGL OF DG PROCESS

Flight height (m)	140 m	160 m	180 m	200 m
Total points	220122	111314	97453	78623
Correct matching points	194629	96776	84519	61325
%Correct matching points	88.42 %	86.94 %	86.73 %	78 %
Wrong matching points	25493	14538	12934	17298
%Wrong matching points	11.58 %	13.06 %	13.27 %	22 %
Average tie point multiplicity	6.385	3.297	2.94	2.63
Matching time	9 hours and 11 minutes	7 hours and 36 minutes	6 hours and 32 minutes	5 hours and 55 minutes

As it is illustrated in table 5, 140 m altitude AGL gives the best matching parameters except matching time. The spare point cloud, correct matching point, and average tie point multiplicity are decreased by increasing altitude AGL. The highest spare point was 220122 points at 140 m with the highest correct matching points 194629 points are reduced to 78623 spare points with 61325 correct matching points at 200 m altitude AGL as the lowest density. Average tie point multiplicity reduced from 6.385 at 140 m AGL as the highest value to 2.63 at 200 m AGL as the lowest value. And the matching time was reduced from 9 hours and 11 minutes at 140 m AGL to 5 hours and 55 minutes at 200 m AGL.

B. The Effect of Overlap Ratio on UAV Images Over Non-Textured Surface:

For assessing the influence of the forward and lateral overlap ratio on processing and generating point clouds of UAV imagery over a featureless surface, three different levels of overlap ratios (60%, 70%, and 80%) flights are processed by the two IG and DG techniques at the same altitude 160 m AGL. The scheme of flights is shown in figure 11. The flight plan consisted of strips working east-west, and the flight planning parameters of the three different overlap ratios are shown in table 6.

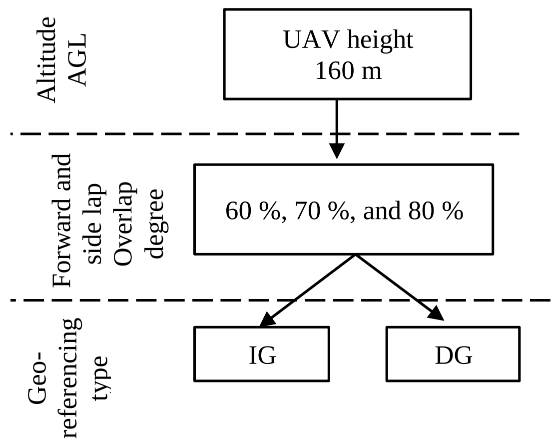

Fig. 11: Scheme of UAV overlap missions and processing.

TABLE 6
THE FLIGHT PLANNING PARAMETERS OF THE FOUR DIFFERENT OVERLAP RATIOS.

Overlap ratio %	**No. of flight lines**	**No. of photos per line**	**No. of total photos**	**Flight time (minutes)**
80	43	30	1290	27
70	29	22	638	14
60	22	17	374	8.5

1. *Study the effect of overlap ratio on IG processing of featureless UAV images:*

The three different overlap ratio flights have been processed by IG using five GCPs and the remaining eight ground points used as ICPs. Figure 5 shows the locations of the GCPs and ICPs. The spatial accuracy assessment is determined by calculating the RMSE of the eight ICPs for easting, northing, and elevation, and the results are shown in table 7 and figure 12.

TABLE 7
THE RMSE OF THE THREE DIFFERENT OVERLAP RATIO OF IG PROCESS.

forward and side overlap	**Flight height (m)**	**GSD (cm/pix)**	**Easting RMSE (m)**	**Northing RMSE (m)**	**Elevation RMSE (m)**	**Total RMSE (m)**
60%	160	3.9	0.11	0.225	0.638	0.685
70%	160	3.9	0.02	0.063	0.105	0.124
80%	160	3.9	0.012	0.028	0.038	0.049

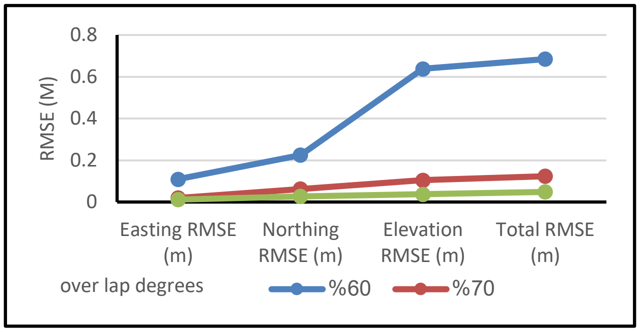

Fig. 12: The correlation between the overlap ratio and RMSE of IG process.

As shown in table 7 and figure 12, the highest overlap ratio recorded the highest spatial accuracy. Decreasing the overlap ratio leads to a decrease in the spatial accuracy of the generated point clouds. 60% overlap recorded 0.685 m spatial accuracy. 70 % overlap gave 0.124 m spatial accuracy. The spatial accuracy of 0.049 m was at 80% overlap.

Besides the spatial accuracy, the matching parameters for the different overlap ratio flights are calculated by the IG process. Table 8 shows the matching parameters for the three missions.

TABLE 8
THE MATCHING PARAMETERS OF THE THREE DIFFERENT OVERLAP RATIOS OF IG PROCESS.

Both forward and side overlap	60%	70%	80%
Total points	57312	78140	141767
Correct matching points	29413	42516	87896
%Correct matching points	51.32 %	54.41 %	62 %
Wrong matching points	27899	35624	53871
%Wrong matching points	48.68 %	45.59 %	38 %
Average tie point multiplicity	2.03	2.19	3.079
Matching time	12 hours and 43 minutes	18 hours and 28 minutes	1 day and 14 hours

From table 8, one can find that 80 % overlap recorded the best matching parameters except matching time. The highest spare point was 141,767 points at 80 % overlap with the highest correct matching points 87,896 points which are reduced to 57312 spare points with 29413 correct matching points at 60 % as the lowest density. Average tie point multiplicity reduced from 3.079 at 80 % overlap as the highest value to 2.03 at 60 % as the lowest value. And the matching time was reduced from 1 day and 14 hours at 80 % overlap to 2 hours and 43 minutes at 60 % overlap.

2. The effect of overlap ratio on DG processing of UAV images over the featureless surface:

For assessing the effect of overlap ratios on the DG process and the spatial accuracy of photogrammetric point clouds, the three different overlap ratios flights (60%, 70%, and 80%) were processed using the known linear EO parameters determined by RTK-GNSS. The eight ICPs were used for assessing the geometric accuracy of the generated point cloud. The RMSE of the eight ICPs were calculated for easting, northing, elevation, and total, shown in table 9 and figure 13.

TABLE 9
THE RMSE OF THE THREE DIFFERENT OVERLAP RATIOS OF DG PROCESS.

Both forward and side overlap	**Flight height (m)**	**GSD (cm/ pix)**	**Easting RMSE (m)**	**Northing RMSE (m)**	**Elevation RMSE (m)**	**Total RMSE (m)**
60%	160	3.9	0.208	0.159	0.348	0.435
70%	160	3.9	0.032	0.026	0.09	0.099
80%	160	3.9	0.018	0.013	0.032	0.039

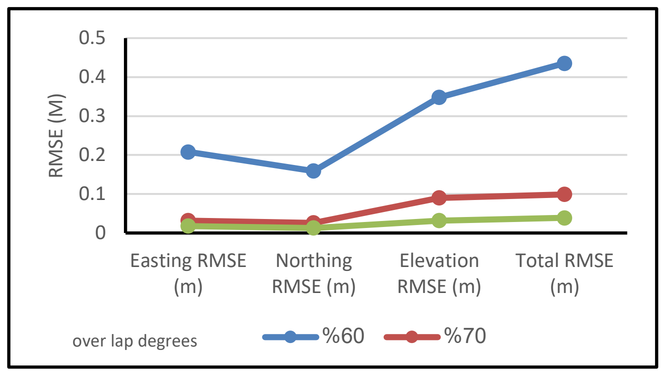

Fig. 13: the correlation between the overlap ratio and RMSE of DG process.

Table 9 and figure 13 show that 80% overlap gave the highest accuracy for the easting, northing, and elevation. From 80% overlap, the mission gave a spatial accuracy of 0.039 m. from 70% overlap, flight gave a geometric accuracy of 0.099 m. the geometric accuracy was 0.435 m with 60% overlap. Reduction overlaps to 70% might be given a suitable spatial accuracy under 0.1 m. reduction the overlap under 70% gave an inappropriate geometric accuracy in topographic applications. The correlation between the overlap ratio and the matching parameters: the spare point density, correct & wrong matching points, average tie point multiplicity, and matching time was calculated and shown in table 10.

TABLE 10
THE MATCHING PARAMETERS OF THE THREE DIFFERENT OVERLAP RATIOS OF DG PROCESS.

Both forward and side overlap	60%	70%	80%
Total points	46752	69015	111314
Correct matching points	35877	56220	96776
%Correct matching points	76.74 %	81.46 %	86.94 %
Wrong matching points	10875	12795	14538
%Wrong matching points	23.26 %	18.54 %	13.06 %
Average tie point multiplicity	2.38	2.79	3.297
Matching time	2 hour and 42 minutes	3 hours and 53 minutes	7 hours and 36 minutes

From table 10, the 80% overlap gave the highest spare point density, highest correct matching points, highest average tie point multiplicity, high matching time, and lowest wrong matching points. At the overlap of 80 %, the largest images number (1290) at a ground sampling distance (resolution) of 3.9 cm/pixel were acquired. The generated point cloud with approximately 111314 3D points was extracted following the DG method.

Generally, the increased image overlap ratio leads to an increase in photogrammetric point clouds' geometric accuracy and matching parameters. The favorable results are obtained for overlap ratios at least 70 % or above in the DG process.

IV. CONCLUSION

This article presented a practical study to use UAV images over featureless surface for topographic mapping. The paper investigates the influence of different flight heights and levels of overlap ratio on the geometric accuracy of the generated topographic mapping products. The results show that the different UAV altitudes 140, 160, 180, and 200 m AGL gave geometric accuracy 0.043, 0.049, 0.052, and 0.057 m for IG process and 0.036, 0.039, 0.048, and 0.053 m for DG process, respectively. The higher ratio of overlap and low flight height recorded the highest spare point clouds, correct matching points, average tie point multiplicity, matching time, and lowest wrong matching point for matching parameters.

Generally, low flight height (140 m) gave high precision with 0.036 m RMSE and the highest reconstruction. The altitude increment might reduce flight time, processing time, and cost while keeping the acceptable geometric accuracy. The increasing of image overlap ratio from 60 % to 80 % leads to an increase in photogrammetric point clouds' geometric accuracy from 0.685m to 0.049 m for IG process. The favorable results are obtained for the four different altitudes and overlap ratios at least 80 % or above.

AUTHORS CONTRIBUTION:

The following summarizes author statement outlining their individual contributions to the paper using the relevant roles:

Ahmed Elhadary: (design of the work, Data collection and tools, Data analysis and interpretation, Funding acquisition, Resources, Methodology, Drafting the article, Critical revision of the article, Final approval of the version to be published)

Mostafa Rabah: (Conception or design of the work, Data collection and tools, Data analysis and interpretation, Project administration, Supervision, Final approval of the version to be published)

Essam Ghanem: (Supervision, Final approval of the version to be published)

Rasha Mohie: (Supervision, Final approval of the version to be published)

Ahmed Taha: (Project administration, Supervision, Final approval of the version to be published)

FUNDING STATEMENT:

The authors received no financial support for the research, authorship and/ or publication of his article.

DECLARATION OF CONFLICTING INTERESTS STATEMENT:

- All authors have participated in (a) conception and design, or analysis and interpretation of the data; (b) drafting the article or revising it critically for important intellectual content; and (c) approval of the final version.
- This manuscript has not been submitted to, nor is under review at, another journal or other publishing venue.
- The authors have no affiliation with any organization with a direct or indirect financial interest in the subject matter discussed in the manuscript

REFERENCES

[1] Aasen, H., Honkavaara, E., Lucieer, E., Zarco-Tejada, P., 2018. Quantitative remote sensing at ultra-high resolution with UAV spectroscopy: a review of sensor technology, measurement procedures, and data correction workflows. Remote Sens., 10, pp. 1091-1933.

[2] Agisoft, 2019. Agisoft Metashape User Manual: Professional Edition, Version1.6. < https://www.agisoft.com/pdf/metashape-pro_1_6_en.pdf>.

[3] Borgogno Mondino, E., Gajetti, M., 2017. Preliminary considerations about costs and potential market of remote sensing from UAV in the Italian viticulture context. Eur. J. Remote Sens., 50, pp. 310-319.

[4] Çelik, M., Aydın A., Bünyan F., Kuşak, L., Kanun, E., 2020. The effect of different flight heights on generated digital products: Dsm and Orthophoto. Mersin Photogrammetry Journal, vol. 2(1), pp. 01-09

[5] Crommelinck, S., Bennett, R., Gerke, M., Ying Yang, M., Vosselman, G., 2017. Contour detection for UAV-Based cadastral mapping. Remote Sens., 9, pp. 171-184.

[6] Daakir, M., Pierrot- Deseilligny, M., Bosser, P., Pichard, F., Thom, C., Rabot, Y., Martin O., 2017. Lightweight UAV with on-board photogrammetry and single-frequency GPS positioning for metrology applications. ISPRS – J. Photogramm., 127, pp. 115-126.

[7] Domingo, Hans Ole Ørka, Erik Næsset, Daud Kachamba and Terje Gobakken, 2019. Effects of UAV Image Resolution, Camera Type, and Image Overlap on Accuracy of Biomass Predictions in a Tropical Woodland. Remote Sens. Vol. 11, pp. 1-17; doi:10.3390/rs11080948.

[8] Falkner, E.; Morgan, D., 2002. Aerial Mapping: Methods and Applications, 2nd ed.; CRC Press: Boca Raton, FL, USA.

[9] FGDC, 1998. Geospatial Positioning Accuracy Standards. FGDC-STD-007.3-1998, Part 3: National Standard for Spatial Data Accuracy (NSSDA).

[10] Manfreda, S., McCabe, M., Miller, P., Lucas, R., Pajuelo Madrigal, V., Mallinis, G., Ben-Dor, B., Helman, D., Estes, L., Ciraolo, G., 2018. On the use of unmanned aerial systems for environmental monitoring. Remote Sens., 10, pp. 641-669.

[11] Mesas-Carrascosa, F. J., Notario García, M. D., Meroño de Larriva, J. E., and García-Ferrer, A., 2016. An Analysis of the Influence of Flight Parameters in the Generation of Unmanned Aerial Vehicle (UAV) Orthomosaicks to Survey Archaeological Areas. Sensors (Basel, Switzerland). 16 (11), 18-38.

[12] Rabah, M., Basiouny, M., Ghanem, E. and Elhadary, A., 2018. Using RTK and VRS in direct geo-referencing of the UAV imagery. NRIAG Journal of Astronomy and Geophysics. 7 (2), 220-226.

[13] Seifert E., Stefan S., Holger V., David D., Jan van A., Anton K. and Thomas S., 2019. Influence of Drone Altitude, Image Overlap, and Optical Sensor Resolution on Multi-View Reconstruction of Forest Images. Remote Sens., vol. 11, 1252; doi:10.3390/rs11101252.

[14] Taha, A., Rabah, M., Mohie, R., Elhadary, A., and Ghanem, E., 2022. Assessment of using UAV imagery over featureless surfaces for topographic applications. Mansoura Engineering Journal. In press.

Title Arabic:

تأثير ارتفاع الطيران والتداخل لصور الطائرات بدون طيار فوق الأسطح المستوية وإنشاء صيغ تتنبأ بالدقة الهندسية لها.

Arabic Abstract:

أدي تطور نظام الطيران بدون طيار (UAS) وخوارزميات الرؤية الحاسوبية (CV) الي التوسع في تقنية التصوير الجوي للحصول على بدائل عالية الدقة ومنخفضة التكلفة لرسم الخرائط للتطبيقات الطبوغرافية. تستخدم خوارزمية (SFM) لتوليد سحب نقطية ثلاثية الأبعاد ونماذج ثلاثية الأبعاد من الصور الجوية المتداخلة. تعد الاسطح المستوية الخالية من المعالم واحدة من أكبر المشاكل التي تعيق الاستخراج الآلي وربط النقاط معا في الصور الجوية. قيمت هذه الورقة البحثية تأثير ارتفاع الطيران ودرجة التداخل بين الصور على الدقة الهندسية لنقاط السحب ثلاثية الأبعاد والنماذج المنتجة من صور الطائرات بدون طيار (UAV) الملتقطة فوق مناطق رملية مستوية. تمت الدراسة باستخدام أربع ارتفاعات طيران مختلفة (140 م، 160 م، 180 م، و200 م) تتعلق بالدقة المكانية (3.41، 3.9، 4.39، 4.68 سم / بيكسل) على التوالي وثلاثة مستويات تداخل مختلفة (60٪، 70٪، و80 ٪) باستخدام صور جوية تم التقاطها بواسطة UX5 UAV فوق منطقة رملية في مدينة الجهراء، الكويت. أظهرت النتائج أن زيادة الارتفاع قد تقلل من زمن الرحلة ووقت المعالجة والتكلفة مع الحفاظ على الدقة الهندسية المقبولة والمناسبة. بشكل عام، يتم الحصول على نتائج مقبولة للارتفاعات الأربعة المختلفة ودرجات التداخل بنسبة 80٪ على الأقل.